

Selective Weighing of Individual Microparticles Using a Hybrid Micromanipulator-Nanomechanical Resonator System

Bin-Da Chan, Kutay Icoz, Richard L. Gieseck, and Cagri A. Savran

Abstract—We report a system based on a combination of a micromanipulator and a cantilever-based differential resonator for selecting and weighing individual micro-scale particles. Instead of relying on probabilistic attachment of particles on sensor surfaces, the system can specifically select and weigh individual micro-entities. The micromanipulator is able to move particles from a native media to the surface of a resonator that can weigh particles with pg-level resolution. The system allows individually manipulating and weighing a wide variety of entities that can be visualized under a microscope, ranging from cell spheres to spore clusters and single diatom algae.

Index Terms—Cantilever, resonator, micro-manipulator, diffraction, stem cell sphere, spore, diatom.

I. INTRODUCTION

CANTILEVER-BASED micro/nano sensors have been used extensively over the past decade to detect a wide variety of entities including biomolecules, chemicals, viruses and cells [1]–[5]. These sensors have been used both in static, i.e. stress sensing, or dynamic, i.e. resonating mode. The latter mode reveals the mass of the target entity by measuring changes in the resonance frequency of the cantilever. Current strategies of weight measurement using cantilevers mostly depend upon probabilistic attachment of the targets on the cantilever surface [6]–[8]. For example, resonators were used to weigh single bacteria and viruses that bind to sensor surfaces both specifically [9] and nonspecifically [10]. Burg *et al.* used suspended microchannel resonators to measure biomolecules and single nanoparticles by flowing the target entities through the inner microchannel of a cantilever [11]. Here, we present a versatile system that allows weighing a wide variety of individual microparticles by discretely

Manuscript received January 25, 2013; revised April 9, 2013; accepted April 18, 2013. Date of publication May 16, 2013; date of current version July 2, 2013. This work was supported by the National Science Foundation under Grant 0925417. The associate editor coordinating the review of this paper and approving it for publication was Prof. Weileun Fang.

B.-D. Chan is with the School of Mechanical Engineering and Birck Nanotechnology Center, Purdue University, West Lafayette, IN 47907 USA (e-mail: chanb@purdue.edu).

K. Icoz and R. L. Gieseck are with Weldon School of Biomedical Engineering and Birck Nanotechnology Center, Purdue University, West Lafayette, IN 47907 USA (e-mail: kutayicoz@gmail.com; rg459@cam.ac.uk).

C. A. Savran is with the School of Mechanical Engineering, Weldon School of Biomedical Engineering, and Birck Nanotechnology Center, Purdue University, West Lafayette, IN 47907 USA (e-mail: savran@purdue.edu).

Color versions of one or more of the figures in this paper are available online at <http://ieeexplore.ieee.org>.

Digital Object Identifier 10.1109/JSEN.2013.2262269

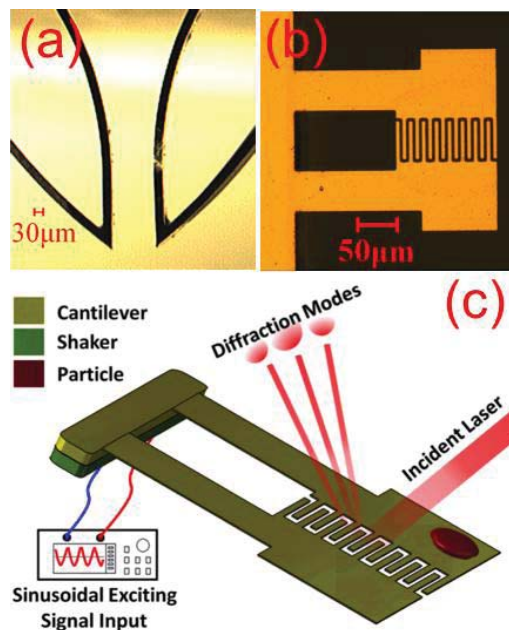


Fig. 1. (a) Micrograph of the micromanipulator's silicon-made tweezer section. (b) The dual-arm nanomechanical resonator. (c) Schematic of the diffractometric measurement strategy.

picking and placing them onto a resonator (similar to a typical weighing scenario in the macro world). The system is based on combining a micromanipulator and a cantilever-based resonator. A single target entity that is selected under a microscope is grabbed by a mechanically-actuated micromanipulator whose fabrication and basic operation have been described previously [12]. The entity is then moved and placed on the tip of the sensor arm of the cantilever for weighing, as seen in Fig. 1.

The system has two adjacent cantilevers, one of which serves as an inherent reference, which suppresses noise and other disturbances that affect both cantilevers similarly. The fabrication of the cantilevers has been described previously [13], [14]. We have fabricated cantilevers with various geometries. The one shown in Fig 1 (the one we make the most use of in this paper), has a length of 250 μm, and a minimum and maximum width of 50 μm and 85 μm, not including the interdigitated fingers which are 5 μm in width and 50 μm in length with 3 μm spacing. The relative motion between the two cantilevers is detected directly by illuminating

the diffraction grating between their tips and measuring the intensity of the reflecting modes [15]–[17].

II. EXPERIMENTAL SETUP

The compact design of the mechanically-actuated micro-manipulator provides mobility and simplicity to manipulate a variety of microparticles in different media [12] and to place them onto the tip of a silicon-nitride cantilever. The gratings are coated with a thin layer of gold to improve reflectivity and are illuminated with a laser beam (Newport R-30091, 5 mW). A photo diode (Thorlabs DET110) is used to measure the intensity of the 0th mode of the reflected diffraction pattern. By analyzing the intensity change of the reflected diffraction mode, the resonance frequencies of both cantilevers can be deduced. Additionally, a piezoelectric shaker (Thorlabs AE0203D04F) is attached below the resonator for excitation [18]. The oscillation amplitude and frequency of the shaker are controlled by a function generator (Tektronix AFG3102). A lock-in amplifier (Stanford Research Systems SR830) is used to record the signal at the excitation frequency. We measure changes in resonance frequency to resolve the loading upon the cantilever, which is expressed by [19]:

$$f = \frac{1}{2\pi} \sqrt{\frac{K}{0.243M + m}}. \quad (1)$$

Here, M is the effective mass of the cantilever, m is the mass of the load and K is the effective stiffness of the cantilever. Accordingly, the difference between the resonance frequencies of the reference and the sensor cantilevers are:

$$\Delta f = \frac{1}{2\pi} \left(\sqrt{\frac{K}{0.243M + m_r}} - \sqrt{\frac{K}{0.243M + m}} \right), \quad (2)$$

where m_r is the added load on the reference cantilever, and m is the added mass on the sensor cantilever. Since the cantilevers are not perfectly rectangular, K and M in (1) and (2) were determined by combining Abaqus finite element simulations with experiments. First, the effective density of a cantilever was taken as 3.65 g/cm³ by averaging a 20 nm thick gold layer with a density of 19.3 g/cm³ [20] and a 480 nm of silicon-rich silicon nitride layer with a density of 3 g/cm³ [21]. The Young's modulus was then estimated to be 182.2 GPa by matching the resonance frequency predicted by the finite element simulation with that observed experimentally (6642 Hz). Next, the K was determined to be 0.0195 N/m using a finite element simulation by applying a vertical point force at the tip and observing the resulting tip deflection. Finally, M was determined to be 46.08 ng by substituting K into (1).

It is known that for maximum sensitivity (i.e., for (1) and (2) to hold), the load needs to be exactly at the tip of the cantilever [22], [23]. Hence, the micromanipulator here also serves the purpose of placing the target load as close to the tip of the cantilever as possible, improving the accuracy of mass measurements. Nevertheless, we do account for the effect of loading location on the resonance frequency. We use finite element analysis to demonstrate the relationship between the resonance frequency, and the location of the loaded particle's center. Fig. 2. shows the variation of the resonance frequency

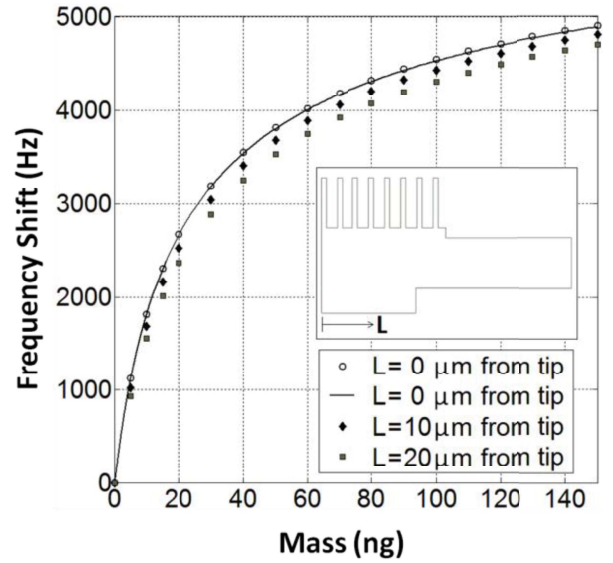


Fig. 2. Variation of resonance frequency with added mass and loading position. The solid curve represents (2) with empty reference cantilever, and data points represent the results of finite element simulations.

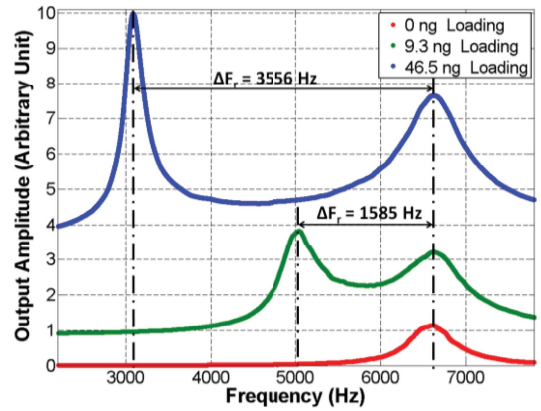


Fig. 3. Frequency response of system for different mass loads. Resonance frequencies of both the sensor and the reference arms are obtained in a single measurement.

shift with different loading masses and locations on the sensor arm. Hence for improved accuracy in determining the mass, we first determine the location of the load using calibrated bright-field microscopy and generate the corresponding frequency shift vs. mass curve using finite element analysis.

Fig. 3 demonstrates the experimental results of frequency response of the system when one of the cantilevers (the sensor arm) is loaded with three different masses. In each experiment, an individual polystyrene bead (Spherotech) with a different mass was placed on the free end of the sensor arm for weighing. Prior to the placement, the micromanipulator was used to dip the bottom of the bead in a small amount of grease. We found that this much grease has negligible mass (~70 pg) in comparison with the particles being weighed and can efficiently improve the adhesion between the particles and the cantilever surface. Further, the grease can be placed directly on the cantilevers (before placing the loads), whose effect on frequencies can be directly accounted for before

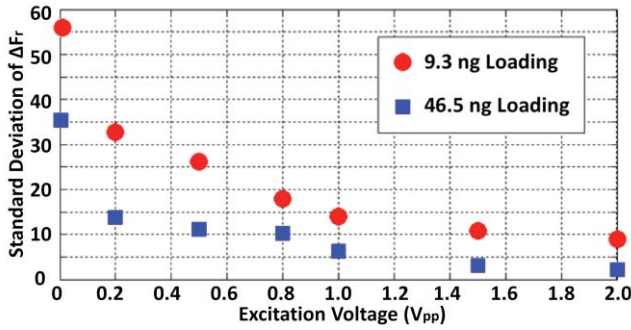


Fig. 4. Dependence of the standard deviation in measured frequency shift on the excitation voltage and loading.

the measurements. In Fig. 3, the frequencies corresponding to the two peaks represent the resonance frequencies of the sensor (low frequency peak) and the reference (high frequency peak) arms. Initially, since both cantilevers are empty, no significant frequency separation occurs and two resonance peaks overlap with each other. As the load on the sensor arm increases, the resonance peak corresponding to the sensor arm shifts to the left and the two resonance frequencies separate. The 46.5 ng and 9.3 ng beads were measured as 12.2 μm and 11.6 μm away from the tip of the cantilever, respectively. The resonance frequency of the reference arm stays unchanged because there is no significant change of mass on the reference arm. The mass of the load on the sensor arm can be derived readily from the frequency separation between the two peaks, with a single measurement. Note that the system can also be used to directly determine the differential mass between two particles by loading both cantilevers (instead of leaving the reference arm empty).

III. DEVICE CHARACTERIZATION

We first examined the repeatability of the resonance frequency measurements. We loaded the sensing cantilever with an individual polystyrene bead with a known mass and varied the peak-to-peak excitation voltage. Two different beads with different masses (9.3 ng and 46.5 ng) were used and each experiment was repeated five times at each excitation voltage. The standard deviation of the measured resonance frequency was then calculated. The results shown in Fig. 4 indicate that the repeatability of the measurements improves both with mass loading and the excitation voltage. This is because the increase in mass improves the quality factor of the cantilever [24], [25], and the external excitation improves the signal-to-noise ratio of the measurement. Hence, in order to reduce the standard deviation of the measured frequency shift, one can place a reference bead of known mass on the reference arm instead of leaving it empty. With this modification, the uncertainty in the resonance frequency can be as low as 1 Hz (our measurement bandwidth), which corresponds to about 3 pg according to (2) with the cantilever mass and stiffness values described above.

We further investigated the effect of other uncertainties on the accuracy of the mass measurement. Since a wafer is fabricated with many devices on it, a user may assume the same properties for all cantilevers on the wafer which can lead

to errors since dimensions could differ slightly. The change in thickness due to non-uniformity of nitride deposition was measured as 8 nm over a distance of 3 inches on a wafer, which for a 500 nm-thick film, could alter the stiffness of a cantilever by 4.9% (cubic dependence on thickness) and its mass by 1.6% (linear dependence on thickness). According to (1), the combined effect of this on a single cantilever's natural frequency (with nominal M of 46.08 ng and K of 0.0195 N/m) would be about 106 Hz. However, due to the differential nature of the system as shown in (2), for small loads up to 2 ng, this effect is suppressed to below 1 Hz (our measurement bandwidth). For a 10 ng load, the uncertainty would be 11 Hz (~ 100 pg).

We also measured that two cantilevers that are 2 inches apart on the wafer can differ in length by as much as 1 μm (possibly due to alignment errors during photolithography). For a 250 μm long cantilever, the effect of this uncertainty on stiffness can be about 1.2%, and on mass 0.4 %, the combined effect of which can be a 53 Hz uncertainty on resonance frequency. However, in a differential system (according to (2)), while measuring small loads (< 290 pg), uncertainty in length results in no detectable error in resonance frequency shift. For a 10 ng load, the uncertainty would be 19 Hz (~ 200 pg).

In practice however, these errors can be mitigated by measuring the dimensions of the particular cantilevers with high accuracy using scanning electron microscopy (SEM) and determining the related M and K before the measurement. For example, a 2 nm uncertainty in measuring thickness in SEM would result in no detectable errors in measuring loads up to 4.7 ng, a 24 pg error in measuring a 10 ng load and a 1.5 ng error in measuring a 100 ng load. A 2 nm uncertainty in 250 μm nominal length would result in no detectable error in resonance frequency. Note that the above uncertainty analyses assumed that the reference cantilever is empty. Hence for a differential system, loading the reference cantilever with a mass similar to that on the sensing cantilever can further mitigate the effects of uncertainties.

We also investigated the effect of uncertainty in the location of the load. An analysis similar to that shown in Fig. 2 suggests that a 200 nm uncertainty in assessing the location of the load (the limit of a typical brightfield microscope) would result in a 23 pg uncertainty in the mass of a 10 ng particle. This uncertainty is less than 3 pg while measuring particles that weigh 1 ng or less. For many applications, this uncertainty can be further mitigated by measuring the location of the load using SEM.

IV. RESULTS AND DISCUSSION

A. Weighing of Individual Stem Cell Spheres

We used the system to weigh individual stem cell spheres. Currently, stem cells are of interest because of their capacity for organ replenishment and for their potential role in cancer initiation and progression [26]–[28]. Stem cells form multiple spheres in soft agar. These spheres are usually not analyzed individually but *en masse* [27]. With the current system an individual stem cell sphere can be extracted from culture medium and weighed. We performed an experiment

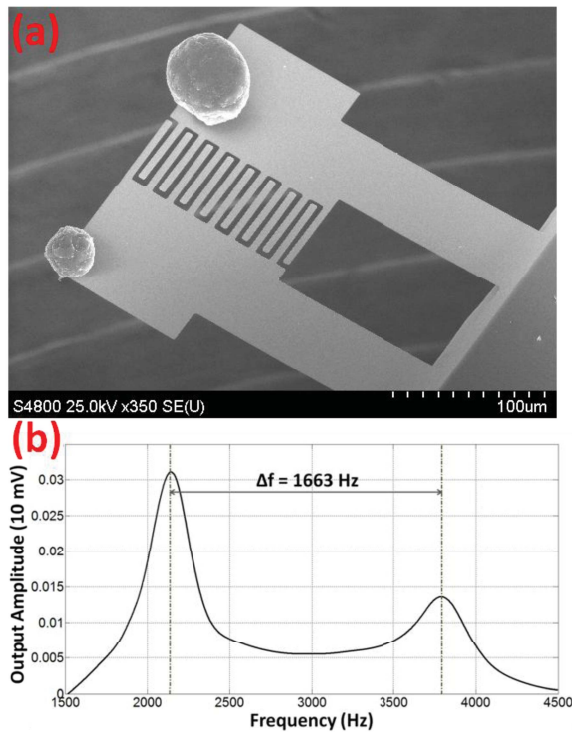


Fig. 5. (a) SEM image and (b) the resulting frequency spectrum showing the comparative weighing of two different stem cell spheres.

with adolescent male murine prostate stem cell spheres that were cultured for 10 days. The cell spheres were fixed by formalin, followed by dehydration using ethanol. Then, the stem cell spheres were left to dry on a glass surface for subsequent testing steps. Fig. 5 illustrates the SEM image of two stem cell spheres placed on different cantilevers for weighing. One of the cantilevers was loaded with a larger stem cell sphere located $14.2 \mu\text{m}$ away from the cantilever tip, while the smaller sphere was located $9.8 \mu\text{m}$ away from the cantilever tip. The left peak and the right peak of the frequency spectrum illustrate the resonance frequencies corresponding to the cantilevers loaded with larger and smaller spheres, respectively. The difference in the masses of both cell spheres is derived as 88.2 ng with the mass of the big cell sphere being 114 ng and small sphere being 25.8 ng . The ability to easily compare two individual stem cell spheres in terms of mass could offer interesting possibilities in understanding their biology and their response to various treatments.

B. Humidity Response of *Bacillus Subtilis* Spores

We also used the system to assess the response of *Bacillus subtilis* spores to environmental stimuli. These spores can absorb water, and dehydrate when heated [29]. By weighing the spores in different humidity levels, the amount of water absorbed by the spores can be measured.

The experiment started by collecting spore clusters using the micromanipulator. After the spores were dried out on a glass surface, the micromanipulator was employed to tenderly pile up the spores. The multilayered coat structure of each spore renders it as one of the most durable cell types [30]. Therefore, the spores remain intact after being grouped. After collecting

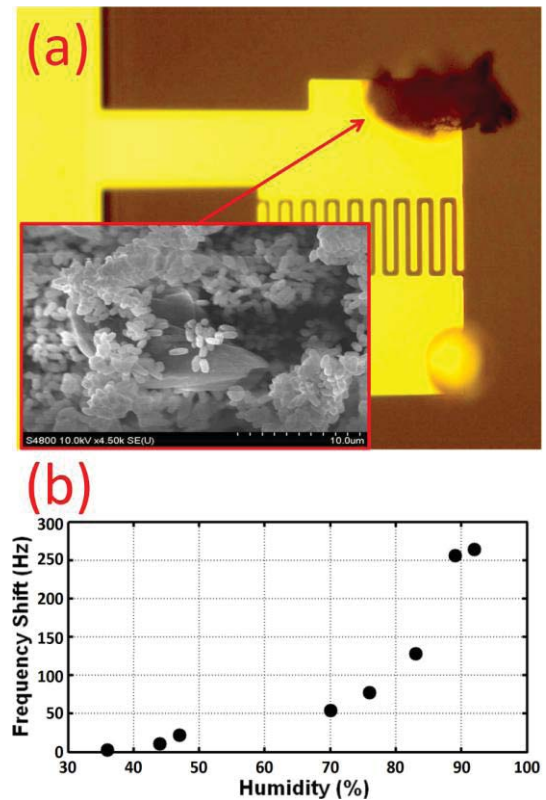


Fig. 6. (a) The micrograph of a spore cluster on one cantilever and a bead on the other. The inset depicts an SEM image of the spores. (b) Change in differential frequency with increasing humidity.

sufficient spores, the cluster of spores was picked up and placed on the tip of the cantilever, which had been pre-paved with a thin layer of grease to prevent the spore cluster from flying away. This particular cantilever pair is slightly different from the one used before hence the effective stiffness and the effective mass were determined again as 0.0187 N/m and 45.6 ng , respectively. As seen in Fig. 6(a), the sensor arm of the cantilever was loaded with a cluster of *B. subtilis* spores, and the reference arm was loaded with a reference bead. The experiment took place in a closed space to facilitate humidity control.

The resulting relationship between humidity change and mass is demonstrated in Fig. 6(b). The initial frequency shift value is deliberately set to 0 for clarity. The initial mass of the spore cluster was 18.8 ng , which varied with relative humidity. The mass increased from 18.8 ng to 23.2 ng as the relative humidity increased from 36% to 92%. The 23.5% increase in the spore mass is in accordance with a previous study [31]. The effect of humidity on the cantilevers themselves is suppressed by the inherently differential detection. Consequently, only the water adsorbed in the spores is measured.

C. Weighing of Diatoms from Pond Water

In order to further test the system's versatility, we used it to weigh individual diatom algae. Diatoms are unicellular algae that are widely observed in aquatic environments. They have been extensively studied in various fields including ecology [32], bioengineering [33], medicine [34], and nanotechnol-

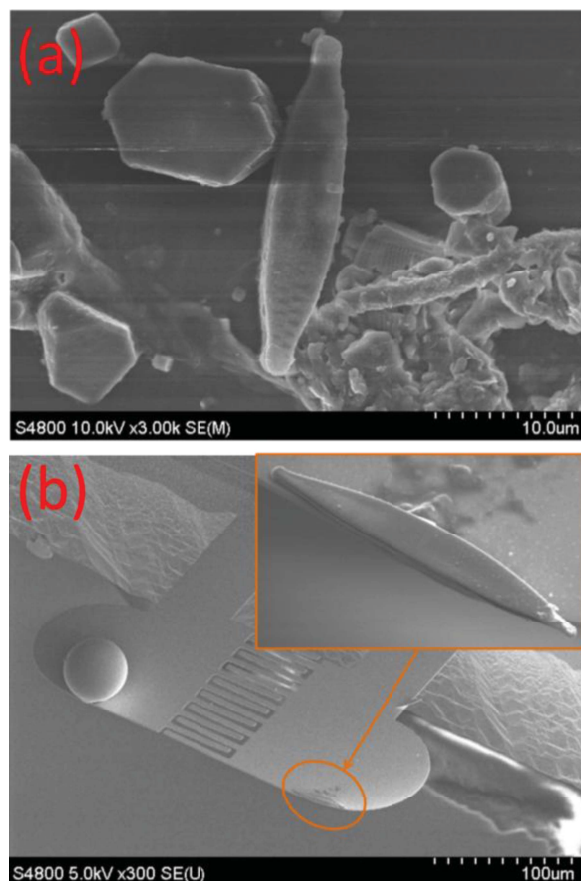


Fig. 7. SEM images of (a) contents of a dried pond water sample and (b) weighing of a diatom selected from the dried sample. The inset depicts a magnified view of the diatom on the cantilever tip.

ogy [35]. Due to their special features such as amorphous silica skeletons, uniform nano-porous structures, chemical inertness, and versatile forms and sizes, researchers have proposed multiple applications of diatoms such as in biophotonics, microfluidics, nanofabrication, gel filtration, and drug delivery [33], [34], [36], [38]. The ability of our system to individually pick and weigh single diatoms could provide new insight into their characterization and their use as biotechnological tools [32].

To measure the mass of diatom particles, a cantilever with circular head shape was used to weigh single diatom cells. The effective stiffness of this particular cantilever pair was 0.0188 N/m and the effective mass was calculated as 54.2 ng. In our experiment, a drop of outdoor pond water that contained large amounts of diverse microorganisms including bacteria, algae, and protozoa, was first left to dry in air on a glass slide. Fig. 7(a) shows a spot on the glass slide with numerous microparticles, a pennate-type diatom [35] and other microorganisms. Using the micromanipulator, we were able to extract a single diatom and place it at the tip of the sensor cantilever for weighing (Fig. 7(b)). Again, a polystyrene bead with known mass was placed on the reference cantilever, to improve the resolution of the measurement. The diatom and the reference bead were placed 2.8 μm and 17.4 μm away from the suspending end of the cantilever, respectively. As a result, the differential resonance frequency between two adjacent cantilevers was measured as 2173 Hz, and the

differential mass between the two particles was measured as 42.2 ng with the mass of the diatom being 4.4 ng.

V. CONCLUSION

We presented a facile and versatile method for selecting and weighing individual microparticles. The system comprises a micromanipulator and a cantilever-based nanomechanical resonator. The use of the mechanically driven micromanipulator can effectively improve the specificity in selecting and analyzing a desired microparticle and allow placement at the tip of the cantilever for accurate mass measurement. The dual cantilever-based resonator is able to directly detect the differential mass between two loads placed on each cantilever individually. With this versatile method, we were able to isolate individual prostate stem cell spheres from culture and measure their weight. The same system was used to aggregate and measure the humidity response of spore cells while minimizing the affect of the humidity on the sensor itself due to the inherently differential nature of the measurement. Lastly, we presented the capability of the system to extract and weigh an individual diatom from a cluster of microparticles found in outdoors pond water.

VI. ACKNOWLEDGMENT

The authors would like to thank the Prof. T. Ratliff Group, Purdue Center for Cancer Research, for providing stem cell spheres.

REFERENCES

- [1] J. Z. Hilt, A. K. Gupta, R. Bashir, and N. A. Peppas, "Ultrasensitive biomems sensors based on microcantilevers patterned with environmentally responsive hydrogels," *Biomed. Microdevices*, vol. 5, pp. 177–184, Sep. 2003.
- [2] K. M. Hansen, H. F. Ji, G. H. Wu, R. Datar, R. Cote, A. Majumdar, and T. Thundat, "Cantilever-based optical deflection assay for discrimination of DNA single-nucleotide mismatches," *Anal. Chem.*, vol. 73, pp. 1567–1571, Apr. 2001.
- [3] R. Flores-Perez, A. K. Gupta, R. Bashir, and A. Ivanisevic, "Cantilever-based sensor for the detection of different chromophore isomers," *Anal. Chem.*, vol. 79, pp. 4702–4708, Jun. 2007.
- [4] N. V. Lavrik, M. J. Sepaniak, and P. G. Datskos, "Cantilever transducers as a platform for chemical and biological sensors," *Rev. Sci. Instrum.*, vol. 75, pp. 2229–2253, Jul. 2004.
- [5] F. M. Battiston, J. P. Ramseyer, H. P. Lang, M. K. Baller, C. Gerber, J. K. Gimzewski, E. Meyer, and H. J. Guntherodt, "A chemical sensor based on a microfabricated cantilever array with simultaneous resonance-frequency and bending readout," *Sens. Actuators B, Chem.*, vol. 77, pp. 122–131, Jun. 2001.
- [6] R. Raiteri, M. Grattarola, H. J. Butt, and P. Skladal, "Micromechanical cantilever-based biosensors," *Sens. Actuators B, Chem.*, vol. 79, pp. 115–126, Oct. 2001.
- [7] K. Park, J. Jang, D. Irimia, J. Sturgis, J. Lee, J. P. Robinson, M. Toner, and R. Bashir, "Living cantilever arrays for characterization of mass of single live cells in fluids," *Lab Chip*, vol. 8, no. 7, pp. 1034–1041, 2008.
- [8] S. Xu and R. Mutharasan, "Rapid and sensitive detection of giardia lamblia using a piezoelectric cantilever biosensor in finished and source waters," *Environ. Sci. Technol.*, vol. 44, pp. 1736–1741, Mar. 2010.
- [9] B. Ilic, D. Czaplewski, M. Zalalutdinov, H. G. Craighead, P. Neuzil, C. Campagnolo, and C. Batt, "Single cell detection with micromechanical oscillators," *J. Vac. Sci. Technol. B*, vol. 19, pp. 2825–2828, Nov.–Dec. 2001.
- [10] A. Gupta, D. Akin, and R. Bashir, "Single virus particle mass detection using microresonators with nanoscale thickness," *Appl. Phys. Lett.*, vol. 84, pp. 1976–1978, Mar. 2004.

- [11] T. P. Burg, M. Godin, S. M. Knudsen, W. Shen, G. Carlson, J. S. Foster, K. Babcock, and S. R. Manalis, "Weighing of biomolecules, single cells and single nanoparticles in fluid," *Nature*, vol. 446, pp. 1066–1069, Apr. 2007.
- [12] B. D. Chan, F. Mateen, C. L. Chang, K. Icoz, and C. A. Savran, "A compact manually actuated micromanipulator," *J. Microelectromech. Syst.*, vol. 21, pp. 7–9, Feb. 2012.
- [13] C. A. Savran, A. W. Sparks, J. Sihler, J. Li, W. C. Wu, D. E. Berlin, T. P. Burg, J. Fritz, M. A. Schmidt, and S. R. Manalis, "Fabrication and characterization of a micromechanical sensor for differential detection of nanoscale motions," *J. Microelectromech. Syst.*, vol. 11, pp. 703–708, Dec. 2002.
- [14] K. Icoz and C. Savran, "Nanomechanical biosensing with immunomagnetic separation," *Appl. Phys. Lett.*, vol. 97, pp. 123701-1–123701-3, Sep. 2010.
- [15] C. A. Savran, T. P. Burg, J. Fritz, and S. R. Manalis, "Microfabricated mechanical biosensor with inherently differential readout," *Appl. Phys. Lett.*, vol. 83, pp. 1659–1661, Aug. 2003.
- [16] C. A. Savran, S. M. Knudsen, A. D. Ellington, and S. R. Manalis, "Micromechanical detection of proteins using aptamer-based receptor molecules," *Anal. Chem.*, vol. 76, pp. 3194–3198, Jun. 2004.
- [17] K. Icoz, B. D. Iverson, and C. Savran, "Noise analysis and sensitivity enhancement in immunomagnetic nanomechanical biosensors," *Appl. Phys. Lett.*, vol. 93, p. 103902, Sep. 2008.
- [18] L. Johnson, A. T. K. Gupta, A. Ghafoor, D. Akin, and R. Bashir, "Characterization of vaccinia virus particles using microscale silicon cantilever resonators and atomic force microscopy," *Sens. Actuators B, Chem.*, vol. 115, pp. 189–197, May 2006.
- [19] D. S. Golovko, T. Haschke, W. Wiechert, and E. Bonaccorso, "Nondestructive and noncontact method for determining the spring constant of rectangular cantilevers," *Rev. Sci. Instrum.*, vol. 78, pp. 043705-1–043705-6, Apr. 2007.
- [20] J. F. Shackelford and W. Alexander, *CRC Materials Science and Engineering Handbook*, 3rd ed. Boca Raton, FL, USA: CRC Press, 2001.
- [21] S. D. Senturia, *Microsystem Design*. Boston, MA, USA: Kluwer, 2001.
- [22] C. J. Liu and E. Bonaccorso, "Microcantilever sensors for monitoring the evaporation of microdrops of pure liquids and mixtures," *Rev. Sci. Instrum.*, vol. 81, pp. 013702-1–013702-8, Jan. 2010.
- [23] N. Lobontiu, I. Lupea, R. Ilic, and H. G. Craighead, "Modeling, design, and characterization of multisegment cantilevers for resonant mass detection," *J. Appl. Phys.*, vol. 103, pp. 064306-1–064306-10, Mar. 2008.
- [24] Y. Liu, G. Zhao, Y. H. Chen, and J. R. Chu, "Size and mass loading effect on quality factor of single-crystal silicon cantilever in atmosphere," in *Proc. 6th Int. Symp. Precis. Eng. Meas. Instrum.*, vol. 7544. 2010, p. 754462.
- [25] Y. Liu, G. Zhao, L. Wen, X. Z. Xu, and J. R. Chu, "Mass-loading effect on quality factor of floppy silicon microcantilever in free air space," *Micro Nano Lett.*, vol. 6, pp. 62–65, Feb. 2011.
- [26] N. Barker, R. A. Ridgway, J. H. van Es, M. van de Wetering, H. Begthel, M. van den Born, E. Danenberg, A. R. Clarke, O. J. Sansom, and H. Clevers, "Crypt stem cells as the cells-of-origin of intestinal cancer," *Nature*, vol. 457, pp. 608–611, Jan. 2009.
- [27] R. U. Lukacs, A. S. Goldstein, D. A. Lawson, D. H. Cheng, and O. N. Witte, "Isolation, cultivation and characterization of adult murine prostate stem cells," *Nature Protocols*, vol. 5, pp. 702–713, Apr. 2010.
- [28] M. F. Clarke, J. E. Dick, P. B. Dirks, C. J. Eaves, C. H. Jamieson, D. L. Jones, J. Visvader, I. L. Weissman, and G. M. Wahl, "Cancer stem cells—perspectives on current status and future directions: AACR Workshop on cancer stem cells," *Cancer Res.*, vol. 66, pp. 9339–9344, Oct. 2006.
- [29] S. Ghosal, T. J. Leighton, K. E. Wheeler, I. D. Hutcheon, and P. K. Weber, "Spatially Resolved Characterization of Water and Ion Incorporation in Bacillus Spores," *Appl. Environ. Microbiol.*, vol. 76, pp. 3275–3282, May 2010.
- [30] V. G. R. Chada, E. A. Sanstad, R. Wang, and A. Driks, "Morphogenesis of Bacillus spore surfaces," *J. Bacteriol.*, vol. 185, pp. 6255–6261, Nov. 2003.
- [31] M. A. Kramer, R. L. Gieseck, B. Andrews, and A. Ivanisevic, "Spore-terminated cantilevers for chemical patterning on complex architectures," *J. Amer. Chem. Soc.*, vol. 133, pp. 9627–9629, Jun. 2011.
- [32] A. Bozarth, U. G. Maier, and S. Zauner, "Diatoms in biotechnology: Modern tools and applications," *Appl. Microbiol. Biotechnol.*, vol. 82, pp. 195–201, Feb. 2009.
- [33] R. Gordon, D. Losic, M. A. Tiffany, S. S. Nagy, and F. A. S. Sterrenburg, "The glass menagerie: Diatoms for novel applications in nanotechnology," *Trends Biotechnol.*, vol. 27, pp. 116–127, Feb. 2009.
- [34] K. M. Wee, T. N. Rogers, B. S. Altan, S. A. Hackney, and C. Hamm, "Engineering and medical applications of diatoms," *J. Nanosci. Nanotechnol.*, vol. 5, pp. 88–91, Jan. 2005.
- [35] J. Bradbury, "Nature's nanotechnologists: Unveiling the secrets of diatoms," *PLOS Biol.*, vol. 2, pp. 1512–1515, Oct. 2004.
- [36] K. H. Sandhage, M. B. Dickerson, P. M. Huseman, M. A. Caranna, J. D. Clifton, T. A. Bull, T. J. Heibel, W. R. Overton, and M. E. A. Schoenwaelder, "Novel, bioclastic route to self-assembled, 3D, chemically tailored meso/nanostructures: Shape-preserving reactive conversion of biosilica (diatom) microshells," *Adv. Mater.*, vol. 14, pp. 429–433, Mar. 2002.
- [37] J. Parkinson and R. Gordon, "Beyond micromachining: The potential of diatoms," *Trends Biotechnol.*, vol. 17, pp. 190–196, May 1999.
- [38] A. R. Parker and H. E. Townley, "Biomimetics of photonic nanostructures," *Nature Nanotechnol.*, vol. 2, pp. 347–353, Jun. 2007.



Bin-Da Chan received the B.S. degree in mechanical engineering from National Chiao Tung University, Hsinchu, Taiwan, in 2006, and the M.S. degree in mechanical engineering from National Taiwan University, Taipei, Taiwan, in 2008. He is currently pursuing the Ph.D. degree in mechanical engineering at Purdue University, West Lafayette, IN, USA, where his doctoral degree focuses on the applications of microsensors and MEMS devices.



Kutay Icoz received the B.S. degree in electronics and communication engineering from Istanbul Technical University, Istanbul, Turkey, in 2002, and the M.S. degree in electrical engineering from Ohio State University, Columbus, OH, USA, in 2004, and the Ph.D. degree in biomedical engineering from Purdue University, West Lafayette, IN, USA, in 2010.

He was a Post-Doctoral Research Associate with the Harvard Medical School and Massachusetts General Hospital, Boston, MA, USA, from 2010 to

2011. Since 2011, he has been a Senior Engineer with the Assembly Test Technology Development Division, Intel Corporation, Chandler, AZ, USA. His current research interests include the development of biomedical sensors and instrumentation for biological signal measurement and recording, and fabrication and characterization of micro-nano devices.



Richard L. Gieseck received the B.S. degree in biomedical engineering from Purdue University, West Lafayette, IN, USA, in 2012. He is currently pursuing the Ph.D. degree at the University of Cambridge, Cambridge, U.K., where he studies under a full NIH Fellowship, and maintains a joint appointment with the National Institute of Allergy and Infectious Diseases.

He is investigating the use of human induced pluripotent stem cells (hiPSCs) to create patient specific, in vitro models of hepatic fibrosis for high-throughput pharmaceutical testing. He is researching the use of hiPSC-derived hepatocytes to ameliorate fibrosis within patients exhibiting late-stage cirrhosis with NIH, Bethesda, MD, USA.



Cagri A. Savran received the B.S. degree in mechanical engineering from Purdue University, West Lafayette, IN, USA, in 1998, and the S.M. and Ph.D. degrees in mechanical engineering from the Massachusetts Institute of Technology, Cambridge, MA, USA, in 2000 and 2004, respectively.

He is currently an Associate Professor of mechanical engineering with Purdue University, with a courtesy appointment in biomedical engineering. His current research interests include the application of MEMS and nanotechnology on biological detection

and manipulation.